JOURNAL OF MATERIALS SCIENCE 17 (1982) 2245–2256

The impact resistance of a ribbon–reinforced composite

Y. T. YEOW*
Research Division, AMP Incorporated, P.O. Box 3608, Harrisburg, Pennsylvania 17105, USA

Utilizing the instrumented impact test system, three test methods are selected to determine the low velocity (1 m sec^{-1}) impact behaviour of a ribbon-reinforced composite, 2826MB/AF147, Metglas–epoxy system. The standard notched Charpy test is used to estimate the inherent impact resistance and the notch sensitivity of the ribbons. The three-point bend test is used to ascertain the influence of the material parameters (ribbon pattern, aspect ratio and orthotropy of the composites) on the dynamic response of four types of laminates. Similarly, the penetration test is used to determine the influence of the material parameters on the response of the composites subjected to localized loading. The results indicate that the test system is capable of disseminating the complete load–time history of the deformation. Subsequently, the variations in the energy-absorbing characteristics of the composites are determined and confirmed by the failure modes of the specimens. Depending on the test method used, the impact resistances of the composites vary according to the mode of loading. However, in each series of tests, the orthotropy of the composite is found to have significant influence on the amount of energy absorbed.

1. Introduction

In recent studies on the behaviour of continuous ribbon-reinforced composites subjected to monotonic loading [1–3], it was found that, due to the rectangular shape of the reinforcement, a composite more capable of being tailored than the ones reinforced with filaments may be obtained. While a knowledge of the basic properties (modulus, strength, Poisson's ratios and fracture strain) is necessary for the effective use of these materials, in reality this information has to be supplemented by additional property data. More specifically, the response of the composites due to impact loading. In such instances, the material response cannot be determined from the basic properties of the materials. Consequently, tests simulating the impact loading conditions would have to be performed in order to determine *a priori* the susceptibility of the composites during service. Thus, the purpose of this study is to determine the dynamic response of a ribbon-reinforced composite subjected to low-velocity impact loading.

In the simulation of the dynamic response of materials, in general, one of the most critical requirements for the proper acquisition of experimental data is in the adoption of the test procedure. In the case of advanced composites, additional considerations are required to take into account the influence of anisotropy on the dynamic response of the materials. Subsequently, three test methods were adopted in this study; namely, the notched Charpy test for thick specimens, the three-point bending test for thin specimens and the penetration test for simulating the response of composite panels due to localized loading. The rationale for these tests is to utilize:

(a) the standard Charpy "V"-notch test, to estimate the inherent impact resistance of the

*Formerly with Allied Corporation, Morristown, NJ, USA.

0022–2461/82/082245–12$03.94/0

reinforcement and to qualitatively determine the notch-sensitivity of the ribbons;

(b) the three-point bend test to determine the material response due to the influence of ribbon aspect ratio (width to thickness), ribbon pattern and orthotropy of the material;

(c) the penetration test to determine the material response due to localized loading and the influence of the material parameters (described in the three-point bend test) on the ease of penetration of the composites.

The main difference between the three-point bend test and the penetration test is in the mode of loading, that is, the former would correspond to uniaxial loading and the latter would correspond to multi-axial loading. Subsequently, the failure modes and impact resistances of the composites are different, as indicated in Sections 4.1 to 4.3 of this work.

It would be appropriate to mention at this juncture that the tests selected for this study are primarily to elucidate the damage of this class of composites. Also, in view of the very limited existing data on this aspect of the composites used here, it is hoped that the data presented herein would be of assistance to the designer, at least on a rule-of-thumb basis. Furthermore, it will be shown that the energy absorbed by the composites is dependent on the constraints of the boundaries.

2. Specimen fabrication

Ribbons of Metglas* 2826MB alloy, an iron–nickel-based alloy, were selected for the reinforcing phase of the composites used in this investigation. The nominal thickness of the ribbons used was 46 μm and two widths, 5.1 and 12.7 mm, were selected. These ribbons were de-greased with methyl–ethyl–ketone solvent, collated and coated with a structural adhesive, AF-147,† in a continous manner. Depending on the spacing between ribbons and/or the width of the ribbon used, the width of the prepregs varied from 150 to 160 mm.

Fig. 1 shows the two types of ribbon pattern used for the laminae, which may consist of two or three layers of ribbons.

The first pattern, denoted as the hexagonal packing (see Fig. 1a), was used to fabricate three types of laminae. The first type contains 5.1 mm wide ribbons, the second and third type contain 12.7 mm wide ribbons. The laminates having these geometries will be referred to, herein, as Type 1, 2 and 3 laminates, respectively. Actual dimensions of the geometries and the ribbon content of the laminae are given in Table I. The geometrical difference between the Type 2 and Type 3 lamina is the ribbon spacing used. Since the former spacing is wider, laminates made from these laminae will have a lower ribbon content.

The second patterns, denoted as the staggered ribbon pattern (see Fig. 1b), is designated as the Type 4 lamina in Table I. The dimensions of the Type 4 lamina are identical to those of the Type 3 lamina except for the stacking of the ribbons.

In order to distinguish the ribbon pattern of the lamina, the orientations of the hexagonal pattern would have a subscript 2 (denoting that the lamina has two layers of ribbons). Similarly, a subscript 3 is used for laminae containing the staggered pattern. Furthermore, unless further specified, laminates fabricated from these laminae would imply unidirectional, cross-ply and their corresponding off-axis orientations.

Using the four types of laminae described above, unidirectional and cross-ply laminates were fabricated. The specimens for three-point bend and penetration tests were obtained from these laminates. The orientations selected for the three-

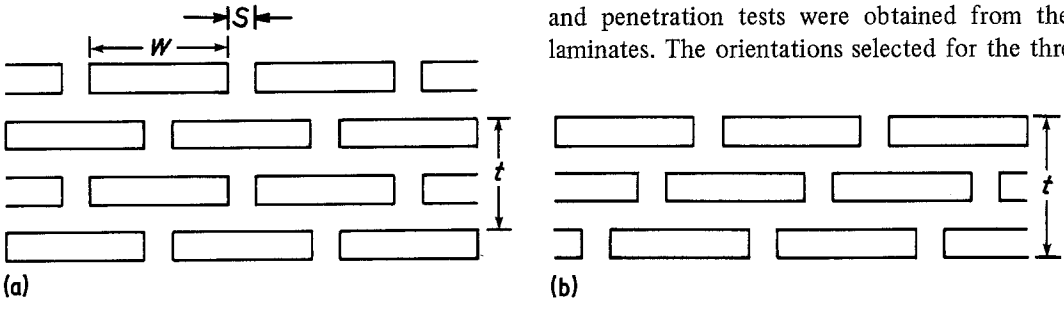

Figure 1 Ribbon pattern used to construct the laminae. The lengths of the ribbons are measured normal to the plane of the figure. (a) $[90^\circ_2]_S$, hexagonal packing and (b) $[90^\circ_3]$, staggered packing.

*Metglas is a registered trade mark of Allied Chemical Corporation.
†AF-147 adhesive manufactured by 3M Company.

TABLE I Lamina construction of 2826MB/AF147 composites

Lamina type	Ribbon width, w (mm)	Spacing, s (mm)	Ribbon content (%)	Lamina thickness, t (mm)
1	5.1	1.27	48	0.13
2	12.7	6.25	43	0.16
3	12.7	2.54	50	0.15
4	12.7	2.54	52	0.23

point bend test specimens were 0°, 45°, 90°, 0°/90°, ± 45° and 90°/0°. These orientations were obtained by measuring the inclusive angles between the length of the ribbons and the longitudinal axis of the specimen. The dimensions of the three-point bend test specimens were 60 mm long by one equivalent width (defined here as the sum of the width of the ribbon and the spacing used) wide. In the case of the Type 1 laminate it was found that a relatively flexible specimen was obtained when one equivalent width was used; thus, the widths were increased to three equivalent widths. The reasons for using the equivalent width criteria in the selection of specimen width have been explained in [4] and will not be repeated here. The geometry selected for the penetration test specimen was 90 mm × 90 mm square panels.

The fabrication procedure for the Charpy "V"-notch specimens consisted of de-greasing the ribbon, sandwiching the adhesive film between layers of 12.7 mm wide ribbons and curing the 410 mm long laminate in an aluminium mould. The overall dimensions of the specimen were 64 mm × 10 mm × 10 mm with a 2 mm deep "V"-notch at the centre of each specimen. Fig. 2 shows the two types of orientations selected for the Charpy tests. The first type, designated as the NL specimen has the ribbons aligned along the span of the specimen and the notch implanted in the direction normal to the ribbons. The second type, designated as the TL specimen, is similar to the NL specimen except that the notch of the TL specimen is implanted in the direction transverse to the ribbons.

3. Experimental procedure

The instrumentation used for this study are the Model 8000 and Model 8200 Dynatup systems.* The maximum capacities of the two machines are 1670 J and 135 J, respectively. These are drop-tower systems which have an instrumented tup that monitors the velocity of the tup before impact and the load–time history of the event. Upon completion of the test, the recorded information is transmitted to a mini-computer and processed. The results, either as load–time and energy–time curves or as load–deflection and energy–deflection curves are displayed and the amount of energy dissipated at various stages of the deformation may then be observed. Further details on the instrumentation and on the calculation of the energy absorbed by the specimen are given in [5–8].

The impact velocity used for all the tests was 1 m sec^{-1}. A span-to-depth ratio of 5 was used for the Charpy specimens. Since a notch was implanted on these specimens and the Charpy test is essentially a beam subjected to three-point bending, the notch of the specimen was either placed on the compressive or tensile side of the beam. Two replicates were used in this series of tests.

In the case of the three-point bend test specimens, the span-to-depth ratio was maintained at 32. This criterion was invoked because of the variation in the thickness of the four types of ribbon pattern selected. Also it was found that this ratio is the minimum ratio required, in order to correspond to the three-point bending properties with the uniaxial tensile properties [9]. Four replicates were used in these tests.

In the penetration tests, a cylindrical tup containing a hemispherical tip was used to penetrate

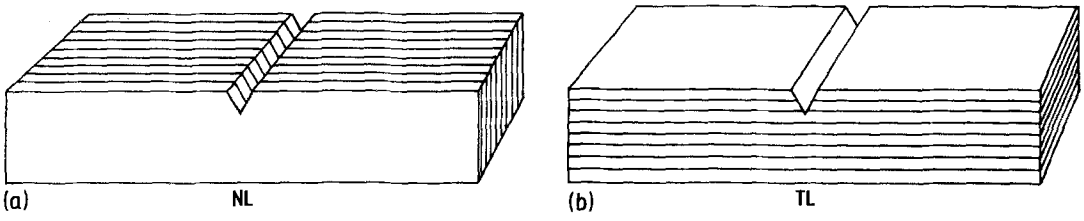

Figure 2 Notched Charpy specimen orientations: (a) Notch normal to the ribbon direction, NL and (b) notch in a direction transverse to the ribbon direction, TL.

*Dynatup systems obtained from Effects Technology, Inc., USA.

the composite. For this series of tests the composite was placed on a cylindrical support (whose centre was aligned to the longitudinal axis of the tup) and lightly clamped on the top with a thin plate containing a hole identical to the support. Again, the centre of the plate was aligned with the centre of the support. The reason for clamping the composite is to prevent the composite from excessive displacement during the impact. Initially, a brief comparative study on the influence of tup diameter and support diameter on the dynamic response of the Type 1 laminates was performed. On the basis of this study, to be described in Section 4.3, the support diameter (63.5 mm) was kept constant and two different tup diameters (12.7 and 25.4 mm) were used. This would permit the determination of the material response due to the influence of the support diameter, D, to tup diameter, d, ratios. Two replicates were used for each D/d ratio determination. In order to qualitatively determine the damage on the composite, the circumference of the tup was drawn on the panel prior to the test.

4. Results and discussion

Typical load and energy response curves obtained from the instrumented test system are shown in Fig. 3. Apart from displaying the complete response, the maximum load, P_{max}, the initiation energy, E_i, or the amount of energy absorbed by the specimen at P_{max}, the total energy absorbed, E_T, by the specimen and the propagation energy, E_P, which is the difference between E_T and E_i, are tabulated in the print-out. All the response measurements presented in this work are based on this data reduction procedure. For some specimens, the values of E_T were corrected in order to eliminate the rebound energy of the tup. The procedure used in these cases is to determine the value of E_T corresponding to the time when P_{max} has decreased by 50% in the event that the load–time curve did not reach the no-load condition or at the first no-load condition.

4.1. Charpy tests

The results of the Charpy tests are presented in Table II where the maximum load, the respective energies and the type of stress (tensile or compressive) imposed on the notch are presented. In the case of the NL Charpy specimen it was found that the nature of the applied stress on the notch has a pronounced effect on the impact behaviour.

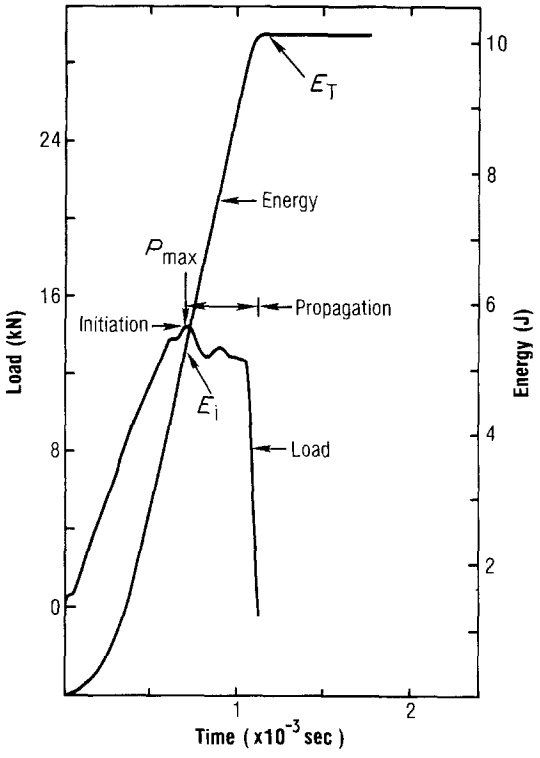

Figure 3 Load and energy response curves for NL Charpy specimen. The notch was placed on the compressive side of the beam.

This effect is further illustrated by Figs 3 and 4 where the complete response of the deformation is shown. Figs 3 and 4 essentially illustrate the notch sensitivity (shown by the variation in P_{max}) and the energy absorbing capabilities (shown by the time required to separate the specimen and the energy curve) of the material. Further confirmation of the notch sensitivity of the NL Charpy specimens was observed in the variation in failure modes. In the case where the notch was subjected to tensile stresses, the fracture surfaces were relatively smooth and a "self-similar"-type of crack propagation was observed (see Fig. 5a). When the notch was subjected to compressive stresses, the fracture surfaces were jagged and slightly inclined to the span of the specimen (see Fig. 5b). The latter failure mode indicate the presence of more energy dissipating mechanisms than the former. Hence, the total impact energy is increased when the notch is subjected to compressive stresses.

Figs 6 and 7 represent the response of the TL Charpy specimens. In the testing of these specimens, especially when the notch was subjected to compressive stresses, rebounding of the tup was observed. Thus, the E_T values are corrected accord-

TABLE II Notched Charpy results for 2826MB/AF147 composites containing 60 vol% ribbon

Orientation	Notch stress state	Load ($\times 10^3$ N)	Energy		
			E_T (J)	E_i (J)	E_P (J)
NL	Tension	8.42	1.63	1.33	0.30
NL	Compression	14.84	9.75	5.33	4.42
TL	Tension	8.14	9.22	7.86	1.36
TL	Compression	9.21	15.73	14.37	1.36

ing to the procedure described above. Again, the influence of the applied stresses at the notch on the impact behaviour of these specimens, similar to the NL specimens, was observed except, for the TL specimens, the variation in P_{max} and the respective energies are not as pronounced as for the NL specimens (see Table II). It would be appropriate to note that when the notch is subjected to tensile stresses, the maximum loads of the NL and TL specimens are similar (Table II), but the amount of energy absorbed is different. This could be attributed to the presence of delaminations (see Fig. 5c) in the TL specimens which is an energy dissipating mechanism. Finally, the failure modes of the TL specimens are similar regardless of the mode of the applied stress on the notch.

4.2. Three-point bend tests

Fig. 8 shows the energy and load response curves of a typical three-point bend test, where "seating-in" of the specimen, occurring when the deflection is between 0 and 0.15 mm, was observed. This behaviour is primarily due to the relatively flexible nature of some of the thin specimens, especially in the case of the Type 1 laminate. Also, due to its lack of rigidity, rebounding of the tup was observed on a number of specimens in this series of tests. The correction procedure, described earlier, is invoked in the determination of the E_T values.

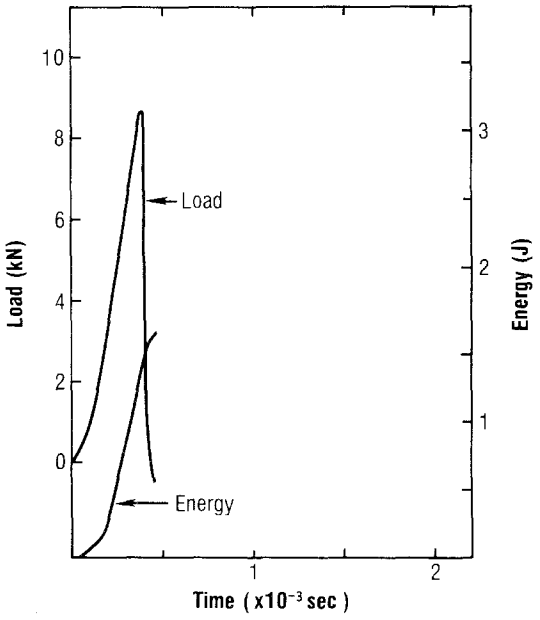

Figure 4 Load and energy response curves for NL Charpy specimen. The notch was placed on the tensile side of the beam.

The averaged values of all the tests are given in Table III. In Table III the strengths of the specimens are calculated from the simple relationship for a three-point bend beam and it is the maximum load that is used in the strength calculations. Since the cross-sectional dimensions of the specimens were varied according to the ribbon pattern, all the energies tabulated in this table are normalized with respect to the cross-sectional area of the specimens, E'_T, E'_i and E'_P. The purpose of the reduction procedure is to provide a more consistent comparison of the response of the laminae used. In terms of strength, the usual orthotropic behaviour (i.e., decreasing strengths with increasing orientation angles) is observed for all the unidirectional laminates. In the case of the cross-ply laminates, the strengths are relatively isotropic, except for the Type 4 90°/0° laminate where a noticeable amount of delamination of the 90° ribbons were observed. Similar trends are observed on the tensile strength of the respective laminates (see Table IV). Quantitatively, since the impact strength of the laminates is always higher than their corresponding tensile strength, such behaviour could be attributed to the time dependent behaviour of the material which, for obvious reasons, will not be studied in this investigation.

In terms of energy, the propagation energy (see Table III) for the majority of the laminates was found to be relatively low and it is difficult to discern the influence of the material parameters (ribbon aspect ratio, ribbon pattern and orthotropy of the material) on the propagation energy. This

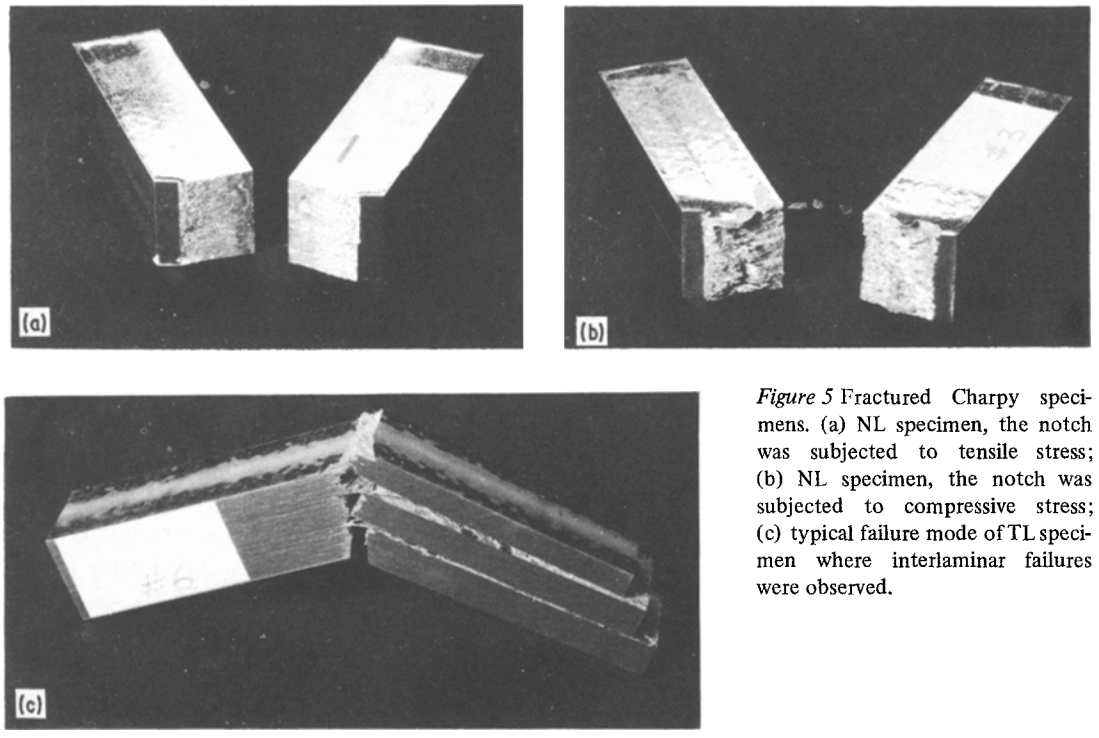

Figure 5 Fractured Charpy specimens. (a) NL specimen, the notch was subjected to tensile stress; (b) NL specimen, the notch was subjected to compressive stress; (c) typical failure mode of TL specimen where interlaminar failures were observed.

could be due to the partial breakages of the specimens, as observed in most of the specimens. The specimens that separated completely are noted in Table III. Fig. 9 shows the typical types of failures

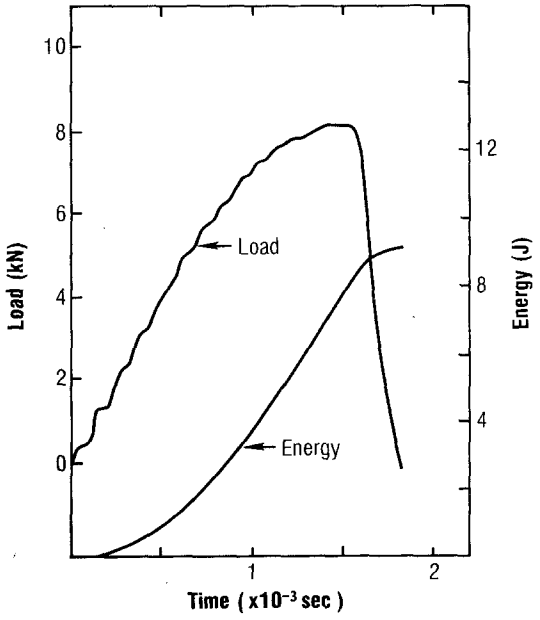

Figure 6 Load and energy response curves of TL Charpy specimen. The notch was placed on the tensile side of the beam.

observed, where the specimens did not separate completely. The number of broken ribbons at the fracture site is not constant. Subsequently, consistent values of the propagation energy are not obtained, in spite of the fact that four replicates were used. An alternative, would be to compare the initiation energy of the various laminates. The results in Table III indicate that the initiation energy is dependent on the orthotropy of the unidirectional laminates and a relatively consistent initiation energy is obtained for the cross-ply and angle-ply laminates. The highest energy is observed in the Type 4 laminates and the lowest energy is observed in the Type 1 laminates.

In retrospect, the impact and tensile results (see Tables III and IV, respectively) indicate that if the tensile strength, modulus and fracture strain of the material are high, such as in the case of the Type 4 laminate, the composite would absorb more energy than in the case of the materials which exhibit lower tensile properties. Also, high impact strength does not necessarily imply high energy absorption. For example, consider the case of the 0° Type 1 and Type 4 laminates where similar failure modes were observed but more energy was absorbed by the 0° Type 4 laminate, in spite of its lower impact strength.

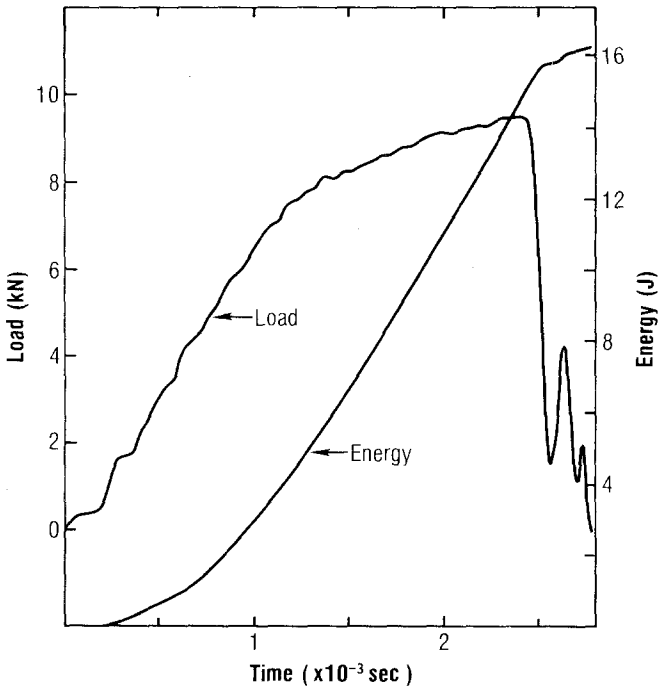

Figure 7 Load and energy response curves of TL Charpy specimen. The notch was placed on the compressive side of the beam.

4.3. Penetration tests

Initially, a brief comparative study on the influence of the support on the impact behaviour of the Type 1 laminate was made. Using a support diameter of 31.8 mm and a penetrator diameter of 12.7 mm, the impact responses of the unidirectional and cross-ply laminates were determined. The results are tabulated in Table V which indicates that, except for E_T and E_P, as expected, the initiation energy of the cross-ply laminate is better than the undirectional laminate. The undirectional laminate has a higher E_T value because the panel separated into two pieces. This resulted in an increase in E_P whereas, in the case of the cross-ply laminate, only localized damage was observed (see Fig. 10). Further observations on the cross-ply laminate revealed that, at the point of entry (see Fig. 10a), the loading was not symmetrical, as indicated by the damaged area relative to the trace of the tup. Subsequently, side-thrusts were generated on the tup which created an uneven damage zone (see Fig. 10b). The primary cause of this discrepancy is the rigidity of the panel. In order to eliminate the problem, the support diameter was increased to 63.5 mm, which resulted in symmetrical loading of the panel (see Fig. 11). The results are presented in Table V. It is interesting to note that the maximum loads of the cross-ply laminates are similar which, in essence, would negate the influence of the support diameter. However, the energies absorbed by the specimens are substantially different.

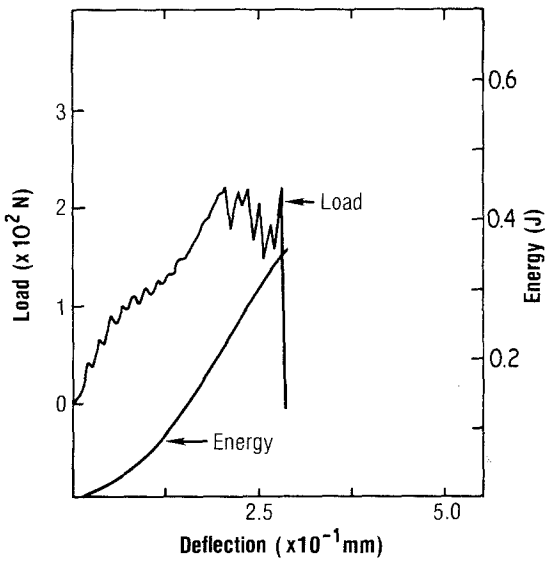

Figure 8 Load and energy response curves of Type 1 $[90_2^\circ]_{2S}$ laminate subjected to three-point bending.

In view of the acceptable results obtained from using a support diameter of 63.5 mm, all the subsequent tests were performed with this support diameter. The results for the Type 2, 3 and 4 laminates which were penetrated with different tup diameters are tabulated in Table VI. The energy densities of the respective laminates are

TABLE III Impact properties of 2826MB/AF147 composites subjected to three-point bend tests

Laminate		Load (N)	Strength (GPa)	Normalized energy		
Type	Orientation			E'_T (J cm^{-2})	E'_i (J cm^{-2})	E'_P (J cm^{-2})
1	$[0^\circ_2]_{2S}$	361*	1.87	4.71	4.46	0.25
1	$[45^\circ_2]_{2S}$	304	1.50	4.07	3.11	0.96
1	$[90^\circ_2]_{2S}$	211	1.10	3.45	2.23	1.22
1	$[0^\circ_2/90^\circ_2]_S$	332	1.64	3.89	3.72	0.17
1	$[90^\circ_2/0^\circ_2]_S$	257	1.33	3.73	2.94	0.79
1	$[\pm 45^\circ_2]_S$	294	1.43	3.60	3.08	0.52
2	$[0^\circ_2]_{2S}$	410	1.55	4.90	4.66	0.24
2	$[45^\circ_2]_{2S}$	380	1.15	3.84	3.54	0.30
2	$[90^\circ_2]_{2S}$	319	1.20	3.83	3.59	0.24
2	$[0^\circ_2/90^\circ_2]_S$	368*	1.51	4.22	4.17	0.05
2	$[90^\circ_2/0^\circ_2]_S$	332	1.40	4.40	3.23	1.17
2	$[\pm 45^\circ_2]_S$	339	1.40	4.10	3.56	0.54
3	$[0^\circ_2]_{2S}$	293	1.56	4.65	3.77	0.88
3	$[45^\circ_2]_{2S}$	288	1.52	4.92	4.29	0.63
3	$[90^\circ_2]_{2S}$	249	1.53	3.41	3.28	0.13
3	$[0^\circ_2/90^\circ_2]_S$	303	1.53	4.49	4.38	0.11
3	$[90^\circ_2/0^\circ_2]_S$	289	1.44	4.64	4.02	0.62
3	$[\pm 45^\circ_2]_S$	282	1.47	5.24	4.30	0.94
4	$[0^\circ_3]_3$	302*	1.66	7.48	6.90	0.58
4	$[45^\circ_3]_3$	307	1.52	6.34	5.88	0.46
4	$[90^\circ_3]_3$	258	1.33	5.30	4.84	0.46
4	$[0^\circ_3/90^\circ_3]_S$	400	1.37	4.65	4.57	0.08
4	$[90^\circ_3/0^\circ_3]_S$	314	1.09	2.98	2.59	0.39
4	$[\pm 45^\circ_3]_S$	425	1.43	5.79	5.57	0.22

*Complete separation of the specimens observed.

obtained by dividing the respective energy, E_T, E_i and E_P, with respect to the areal volume (defined here as the product of the cross-sectional area of the tup and the thickness of the laminate) of the localized damage. This normalization procedure is used primarily for comparative purposes. As expected, the results indicate that the maximum load and energy absorbed are higher when the large tup was used. The reduction in rupture load when the smaller tup was used is approximately one third less than the rupture load of the larger tup, for all the laminates. This behaviour would imply that the dynamic rupture strength is dependent on the diameter of the tup. In terms of

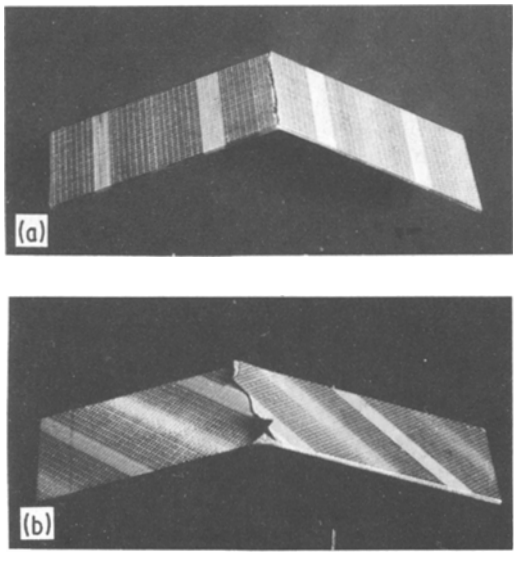

Figure 9 Fractured Type 3 specimens subjected to three-point bending. Delaminations were observed on all specimens containing 45° laminae. (a) $[90^\circ_2]_{2S}$, (b) $[45^\circ_2]_{2S}$ and (c) $[\pm 45^\circ_2]_S$.

TABLE IV Tensile properties of 2826MB/AF147 composites

Laminate		Axial strength (GPa)	Axial modulus (GPa)	Fracture strain (%)	Poisson's ratio
Type	Orientation				
1	$[0^\circ_2]_{2S}$	1.39	88.6	1.62	0.34
1	$[45^\circ_2]_{2S}$	0.84	81.1	1.40	0.33
1	$[90^\circ_2]_{2S}$	0.71	80.3	0.98	0.32
1	$[0^\circ_2/90^\circ_2]_S$	1.00	83.2	1.65	0.31
1	$[90^\circ_2/0^\circ_2]_S$	0.99	79.6	1.61	0.28
1	$[\pm 45^\circ_2]_S$	0.94	79.2	1.70	0.33
2	$[0^\circ_2]_{2S}$	1.15	81.1	1.62	0.32
2	$[45^\circ_2]_{2S}$	0.86	76.1	1.37	0.31
2	$[90^\circ_2]_{2S}$	0.84	70.4	1.61	0.27
2	$[0^\circ_2/90^\circ_2]_S$	0.99	75.1	1.48	0.30
2	$[90^\circ_2/0^\circ_2]_S$	0.98	75.0	1.51	0.29
2	$[\pm 45^\circ_2]_S$	0.97	74.2	1.49	0.35
3	$[0^\circ_2]_{2S}$	1.13	83.0	1.43	0.31
3	$[45^\circ_2]_{2S}$	0.83	79.0	1.46	0.33
3	$[90^\circ_2]_{2S}$	0.75	67.3	1.50	0.26
3	$[0^\circ_2/90^\circ_2]_S$	1.05	72.2	1.59	0.25
3	$[90^\circ_2/0^\circ_2]_S$	1.17	74.2	1.65	0.26
3	$[\pm 45^\circ_2]_S$	0.92	71.1	1.37	0.31
4	$[0^\circ_3]_3$	1.42	91.2	1.80	0.32
4	$[45^\circ_3]_3$	0.99	83.4	1.57	0.36
4	$[90^\circ_3]_3$	1.02	82.5	1.60	0.29
4	$[0^\circ_3/90^\circ_3]_S$	1.24	85.0	1.57	0.30
4	$[90^\circ_3/0^\circ_3]_S$	1.15	85.9	1.54	0.32
4	$[\pm 45^\circ_3]_S$	1.13	82.9	1.54	0.30

energy density, the variation in the tup diameter would vary the initiation energy density, E_i^*, by two or three times. The variation in the total energy density, E_T^*, and propagation energy density, E_P^*, with respect to the change in tup diameter will not be discussed because the rupture of the specimens was affected by the presence of the frictional forces which were created by the grabbing of the fracture surface onto the cylindrical section of the tup. Consequently, the two energy terms, E_P^* and E_T^*, would have to be corrected in order to account for this discrepancy. Due to the unknown nature of the frictional energy, no correction was made.

A typical failure mode observed on the Types 1, 2 and 3 laminates penetrated with the 25.4 mm diameter tup is that, when the axial to longitudinal (0° laminate) tensile strength ratio of the laminate is $\simeq 65\%$ or less, the specimen would split into two pieces. For strength ratios greater than 65%, only localized damage was observed. Figs 12 and 13 show the influence of tup diameter on the damage of the composites. A relative measure of the damage may be obtained by comparing the size of the damage and the trace of the tup. In the case when the 12.7 cm diameter tup was used, the cracks always propagate into the spacing of the ribbons (see Fig. 12). When the larger tub was used, the fracture is more catastrophic (see Fig. 13) and the number of ribbon breakages is increased. This, in turn, increased the energy absorbed by the composite.

TABLE V Impact properties of 2826MB/AF147 composites, of laminate Type 1, subjected to penetration

Laminate		Support diameter (mm)	Penetrator diameter (mm)	Load (N)	Energy		
Type	Orientation				E_i (J)	E_T (J)	E_P (J)
1	$[0^\circ_2]_{2S}$	31.8	12.7	469	0.35	0.80	0.45
1	$[0^\circ_2/90^\circ_2]_S$	31.8	12.7	684	0.47	0.75	0.28
1	$[0^\circ_2/90^\circ_2]_S$	63.5	12.7	682	0.61	1.15	0.54

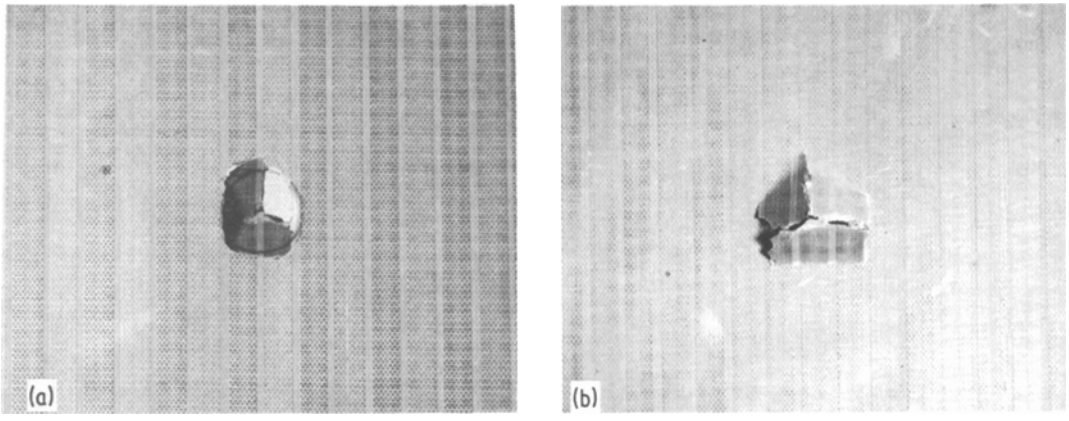

Figure 10 Type 1 $[0_2^\circ/90_2^\circ]_s$ panel subjected to localized loading; (a) top and (b) bottom. The diameter of the tup and support used are 12.7 mm and 63.8 mm, respectively. Note the uneven rupture at the bottom side of the specimen.

On a comparative basis, the results (Table VI) indicate that the Type 4 cross-ply laminate exhibits the best resistance to penetration and an appreciable difference is observed between the Types 2 and 3 laminates. Similar conclusions may be made on the tensile properties (Table IV) of the latter laminates. Due to the influence of the boundary conditions and tup diameter on the response of the composites, comparisons of the penetrability of the composites used here with other materials were not made.

5. Conclusions

The test system used in this study was found to be suitably convenient for determining the dynamic response of the composites. Whatever discrepancy and/or disparity observed on the failed specimens or boundary conditions observed are clearly indicated in the load–time and energy–time response curves. Subsequently, the influence of the orthotropy of the composites, ribbon pattern and aspect ratio of the impact resistance of the composites are identified.

The results of the notched Charpy specimens indicate that the orthotropy of the material has significant influence on its dynamic response. This is substantiated by the variation in the energy absorbed and the maximum load imposed on the NL and TL Charpy specimens. Of the two orientations selected, the NL specimens were found to be more notch sensitive than the TL specimens and, due to the presence of delaminations, the TL specimens absorbed more energy than the NL specimens.

The normalized three-point bend test results indicate that the impact strength and initiation

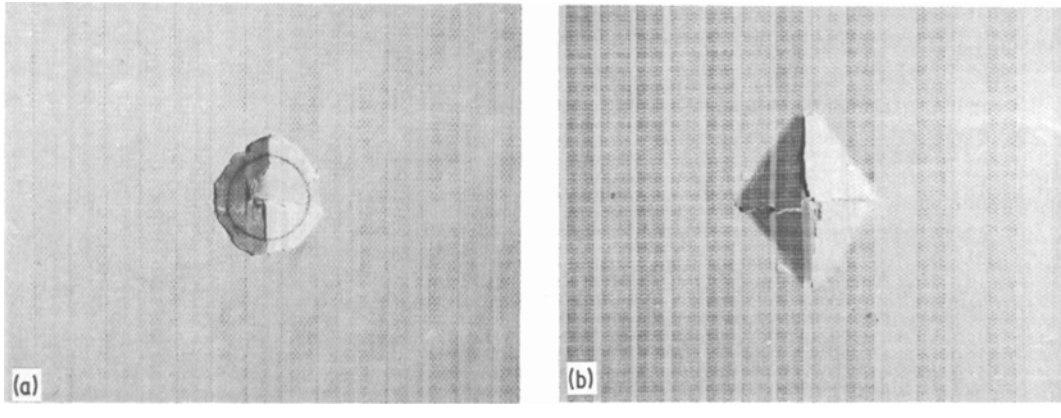

Figure 11 Type 1 $[0_2^\circ/90_2^\circ]_s$ panel subjected to localized loading; (a) top and (b) bottom. The diameter of the tup and support used are 12.7 mm and 63.5 mm, respectively. Homogeneous rupture was observed on both sides of the specimen.

TABLE VI Impact properties of 2826MB/AF147 composites, of laminate Types 2, 3 and 4, subjected to penetration. The diameter of the support was 63.5 mm

Laminate		Penetrator diameter (mm)	Load ($\times 10^3$ N)	E_T (J)	E_i (J)	Energy density		
Type	Orientation					E_T^* (J cm^{-3})	E_i^* (J cm^{-3})	E_P^* (J cm^{-3})
2	$[0_2^\circ]_{2S}^\dagger$	25.4	1.06	3.08	1.08	9.20	3.23	5.97
2	$[0_2^\circ/90_2^\circ]_S$	12.7	0.75	1.97	0.79	24.99	10.23	14.76
2	$[0_2^\circ/90_2^\circ]_S$	25.4	1.17	2.03	1.19	6.44	3.77	2.67
3	$[0_2^\circ]_{2S}$	12.7	0.75	1.86	0.75	24.09	9.71	14.38
3	$[0_2^\circ]_{2S}^\dagger$	25.4	1.42	4.42	1.06	14.31	3.43	10.88
3	$[0_2^\circ/90_2^\circ]_S$	12.7	0.80	1.55	0.77	20.07	9.97	10.10
3	$[0_2^\circ/90_2^\circ]_S$	25.4	1.40	2.41	1.53	7.80	4.95	2.85
4	$[0_3^\circ]_3$	12.7	0.97	2.07	1.00	21.44	10.36	11.08
4	$[0_3^\circ]_3$	25.4	1.54	2.62	1.41	6.79	3.65	3.14
4	$[0_3^\circ/90_3^\circ]_S$	12.7	1.04	5.29	1.63	43.84	13.51	30.33
4	$[0_3^\circ/90_3^\circ]_S$	25.4	1.73	6.36	4.46	13.18	4.29	8.89

energy of the unidirectional laminates are influenced by the orthotropy of the material. Due to the relatively isotropic in-plane properties of the cross-ply laminates, the impact strength and initiation energy exhibit mild dependence on the directionality of the ribbons. The 0°/90° and 90°/0° results show that the former stacking sequence exhibits higher impact strength and initiation energy than the latter. This is primarily due to the delamination of the 90° laminae in the 90°/0° laminate. It was observed that the majority of the specimens did not separate into two pieces and the number of broken ribbons in each series of tests was found to vary. Thus, consistent values of the propagation energy and total energy absorbed are not obtained. The trends of the impact results are similar to the tensile results of the respective laminates.

The penetration test results indicate that the cross-ply laminates absorb more energy than the undirectional laminates. This is primarily due to the better biaxial properties of the cross-ply laminates. The initiation energy and maximum load of all the laminates were found to be dependent on the diameter of the tup. However, the variations of these properties are not proportional to the changes in diameter of the tup. Similar behaviour is observed for the initiation energy density of the laminates used.

In conclusion, this study shows that in order to increase the energy absorbing capabilities of a material the tensile properties of the material, such as modulus, strength and fracture strain, would have to be increased. In the case of advanced composites, due to its ease of tailoring, these three parameters would have to be optimized. The

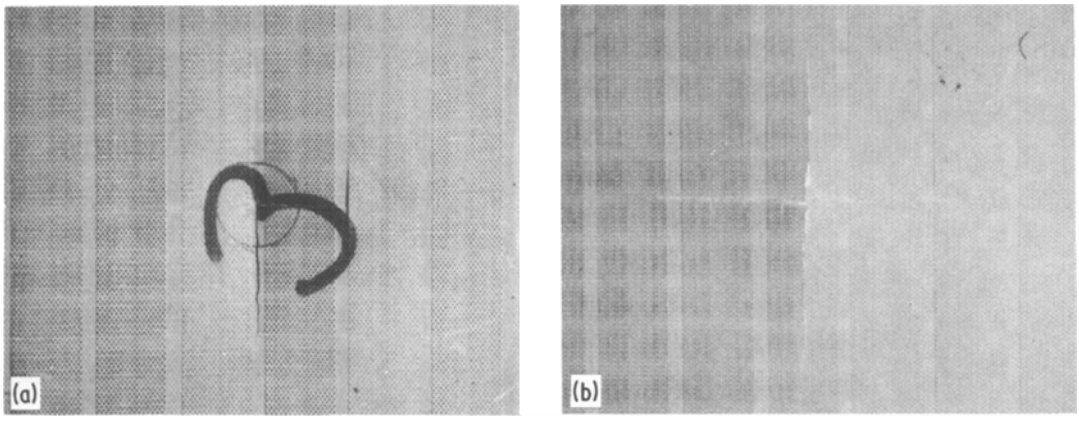

Figure 12 Type 3 $[0_2^\circ/90_2^\circ]_S$ panel subjected to localized loading; (a) top and (b) bottom. The diameter of the tup used was 12.7 mm.

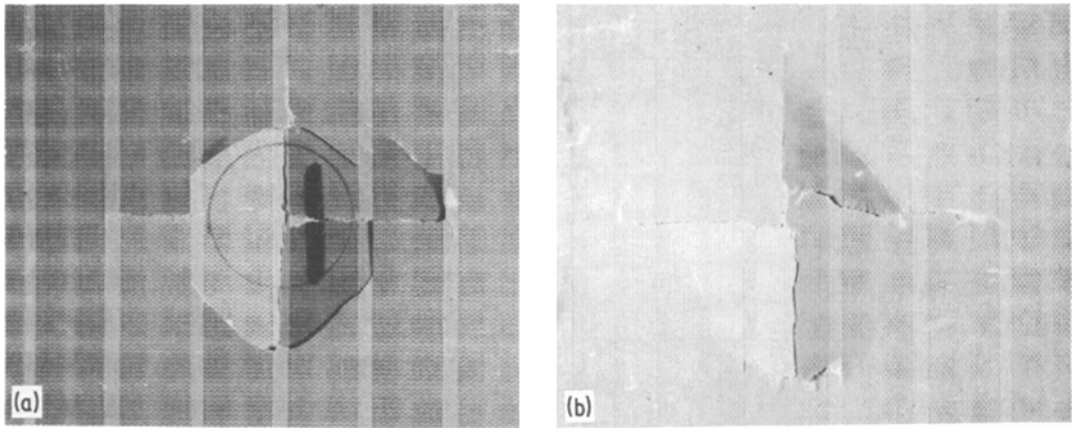

Figure 13 Type 3 $[0_2^\circ/90_2^\circ]_S$ panel subjected to localized loading; (a) top and (b) bottom. The diameter of the tup used was 25.4 mm.

results of the three-point bend and penetration tests show that, for similarly oriented laminates, the Type 4 laminates have the best impact resistance. Upon comparing the tensile properties of the composites, the Type 4 laminates exhibit the highest tensile modulus, strength and fracture strain. Further comparisons of the results of other materials [10] show that materials having well balanced tensile properties are normally impact resistant. Unfortunately, to the author's knowledge, detailed quantitative studies on the influence of the respective parameters on the impact behaviour of materials are not available in the literature.

Acknowledgements

The author would like to express his gratitude and sincere appreciation to Mr D. Timan for his assistance, Mr A. Freilich for supplying the ribbons, Mr J. Schurb and his associates at 3M Company for their co-operation, Mr K. Lew at Effects Technology Inc., for performing the tests and Ms C. Storzum for typing the report.

References

1. Y. T. YEOW, *J. Composite Mater. Suppl.* **14** (1980) 132.
2. *Idem, Composites* **12** (1981) 139.
3. J. R. STRIFE and K. M. PREWO, Proceedings of the 11th National SAMPE Technical Conference, Boston, Massachusetts, November 1979 (S.P.E., Brookfield Center, Connecticut, 1979) p. 286.
4. Y. T. YEOW, Paper presented at the 6th ASTM Conference on Composite Materials: Testing and Design, Phoenix, Arizona, May 1981 (A.S.T.M., Philadelphia, Pennsylvania, in press).
5. R. H. TOLAND, Proceedings of the Failure Modes in Composites Symposium, AIME Spring Meeting, Boston, Massachusetts, May 1972 (A.I.M.E., Warrendale, Pennsylvania, 1972) p. 386.
6. D. F. ADAMS and A. K. MILLER, *Mater. Sci. Eng.* **19** (1975) 245.
7. P. K. MALLICK and L. J. BROUTMAN, *J. Testing Evaluation* **5** (1977) 190.
8. J. C. ALESZKA, *ibid.* **6** (1978) 202.
9. C. ZWEBEN, W. S. SMITH and M. W. WARDLE, ASTM Special Technical Publication, number ASTM-STP-674 (ASTM, Philadelphia, Pennsylvania, 1979) p. 228.
10. D. F. ADAMS and A. K. MILLER, *Mater. Sci. Eng.* **19** (1975) 245.

Received 9 November
and accepted 15 December 1981